Supplemental Material: Efficient multiphoton sampling of molecular vibronic spectra on a superconducting bosonic processor

Christopher S. Wang,[1,2,*] Jacob C. Curtis,[1,2] Brian J. Lester,[1,2] Yaxing Zhang,[1,2] Yvonne Y. Gao,[1,2] Jessica Freeze,[3] Victor S. Batista,[3] Patrick H. Vaccaro,[3] Isaac L. Chuang,[4] Luigi Frunzio,[1,2] Liang Jiang,[1,2,†] S. M. Girvin,[1,2] and Robert J. Schoelkopf[1,2,‡]

[1] *Departments of Physics and Applied Physics, Yale University, New Haven, CT 06511, USA.*

[2] *Yale Quantum Institute, Yale University, New Haven, CT 06520, USA.*

[3] *Department of Chemistry, Yale University, New Haven, CT 06511, USA.*

[4] *Department of Physics, Center for Ultracold Atoms, and Research Laboratory of Electronics, Massachusetts Institute of Technology, Cambridge, MA 02139, USA.*

* christopher.wang@yale.edu

† current address: Pritzker School of Molecular Engineering, University of Chicago, Chicago, IL 60637, USA.

‡ robert.schoelkopf@yale.edu

I. NUMERICAL FRANCK-CONDON DATA

Additional experimental data is provided in this section. TABLE I provides an overview of the different molecular processes that are simulated and corresponding information regarding post-selection, systematic offsets, and distance metrics.

The data for each molecular process in the following tables is calculated as follows. For the "single-bit extraction" scheme, the probability and standard error for a given joint photon number of interest is:

$$q_{n',m'}^{\text{meas}} = \frac{n_{n',m'}^{ee}}{N_{n',m'}^{\text{runs}}} \tag{S33}$$

$$\sigma_{n',m'} = \sqrt{\frac{q_{n',m'}^{\text{meas}}(1 - q_{n',m'}^{\text{meas}})}{N_{n',m'}^{\text{runs}}}} \tag{S34}$$

where $n_{n',m'}^{ee}$ is the number of counts where both ancillas are measured in their excited state, indicating a measure for population in $|n', m'\rangle$ (see Eq. 4 in the main text), and $N_{n',m'}^{\text{runs}}$ is the total number of runs of the experiment for probing $|n', m'\rangle$. The number of runs varies slightly among different final states due to varying post-selection probabilities. The correction protocol outlined in Appendix E of the main text is then applied to $q_{n',m'}^{\text{meas}}$ to retrieve a new probability distribution $p_{n',m'}^{\text{meas}}$. The standard error $\sigma_{n',m'}$ is truncated to one significant digit and $p_{n',m'}^{\text{meas}}$ is then rounded to the precision set by $\sigma_{n',m'}$. The data reported is $p_{n',m'}^{\text{meas}} \pm \sigma_{n',m'}$ only for probabilities with significant support relative to the precision of the experiment ($p_{n',m'}^{\text{ideal}} \gtrsim 10^{-4}$).

The same method (sans the correction protocol) is applied to the data for the "sampling" scheme, except there the probabilities and standard error are given by:

$$q_{n',m'}^{\text{meas}} = \frac{n_{n',m'}}{N_{\text{runs}}} \tag{S35}$$

$$\sigma_{n',m'} = \sqrt{\frac{q_{n',m'}^{\text{meas}}(1 - q_{n',m'}^{\text{meas}})}{N_{\text{runs}}}} \tag{S36}$$

where $n_{n',m'}$ is the number of times the joint photon number $|n', m'\rangle$ is sampled from the total number of runs of the experiment N_{runs}.

Sometimes, there will be no counts reported for a given $|n', m'\rangle$ (i.e., $n_{n',m'}^{ee}$ or $n_{n',m'} = 0$). In this case, we simply report a probability of zero. Furthermore, sometimes the correction protocol will return negative elements in the probability distribution due to statistical noise; these unphysical cases are also nulled and a zero is reported. All distances $D = \frac{1}{2}\sum_{i=0}^{n_{\max}}\sum_{j=0}^{n_{\max}} |p_{ij}^{\text{meas}} - p_{ij}^{\text{ideal}}|$ are calculated after this correction process, with the corresponding values for $n_{\max}$ specified in TABLE I.

Full time-domain master equation simulations are performed using QuTiP and consider only the Hilbert space of the two cavities with $n_{\max} = 30$. Each Gaussian operation is simulated by evolving the associated Hamiltonian term, while also including the corresponding self-Kerr terms and photon loss for each operation. While squeezing cavity A, for instance, the native self-Kerr and photon loss rates for cavity B are used, assuming that the pumped process for squeezing cavity A does not change the participation of cavity B in any nonlinear lossy modes (and vice-versa). The simulation also takes into account photon loss during the verification measurement, which takes 2.5 μs. The simulation does not consider imperfect state preparation and systematic errors in calibrations, which we believe to account for the remaining difference between the measured distances for the "single-bit extraction" scheme and predicted distances from the master equation simulations.

Molecular transition	Initial state (n, m)	Percentage of data kept	$n_{\max}$	t_A, t_B f_A, f_B	Distance to ideal distribution			Figure
					Single-bit extraction	Sampling	Master Equation	
$H_2O \xrightarrow{h\nu} H_2O^+(\tilde{B}^2B_2) + e^-$	$(0,0)$	$\sim 95\%$	16	0.937, 0.946 0.005, 0.002	0.049(1)	0.151(9)	0.0123	FIG. 7
$O_3^- \xrightarrow{h\nu} O_3 + e^-$	$(0,0)$	$\sim 96\%$	12	0.937, 0.948 0.005, 0.002	0.039(9)	0.075(2)	0.0052	FIG. 8
	$(1,0)$	$\sim 95\%$	10	0.937, 0.950 0.004, 0.002	0.057(5)	0.085(5)	0.0131	FIG. 9
	$(1,2)$	$\sim 93\%$	12	0.938, 0.950 0.004, 0.001	0.105(3)	0.148(4)	0.0217	FIG. 10
$NO_2^- \xrightarrow{h\nu} NO_2 + e^-$	$(0,0)$	$\sim 94\%$	12	0.935, 0.943 0.005, 0.003	0.034(0)	0.110(9)	0.0331	FIG. 11
	$(1,0)$	$\sim 92\%$	14	0.934, 0.951 0.004, 0.002	0.202(2)	0.209(7)	0.1269	FIG. 12
$SO_2 \xrightarrow{h\nu} SO_2^+ + e^-$	$(0,0)$	$\sim 96\%$	12	0.938, 0.950 0.004, 0.002	0.019(6)	0.095(3)	0.0065	FIG. 13
	$(0,1)$	$\sim 94\%$	12	0.931, 0.951 0.004, 0.001	0.063(7)	0.136(6)	0.0213	FIG. 14

TABLE I. **Summary of experimental data.** List of molecular processes simulated and corresponding post-selection probabilities, maximum photon number probed with the "single-bit extraction" measurement scheme, and distances. Transmon offsets are independently measured after each dataset is taken.

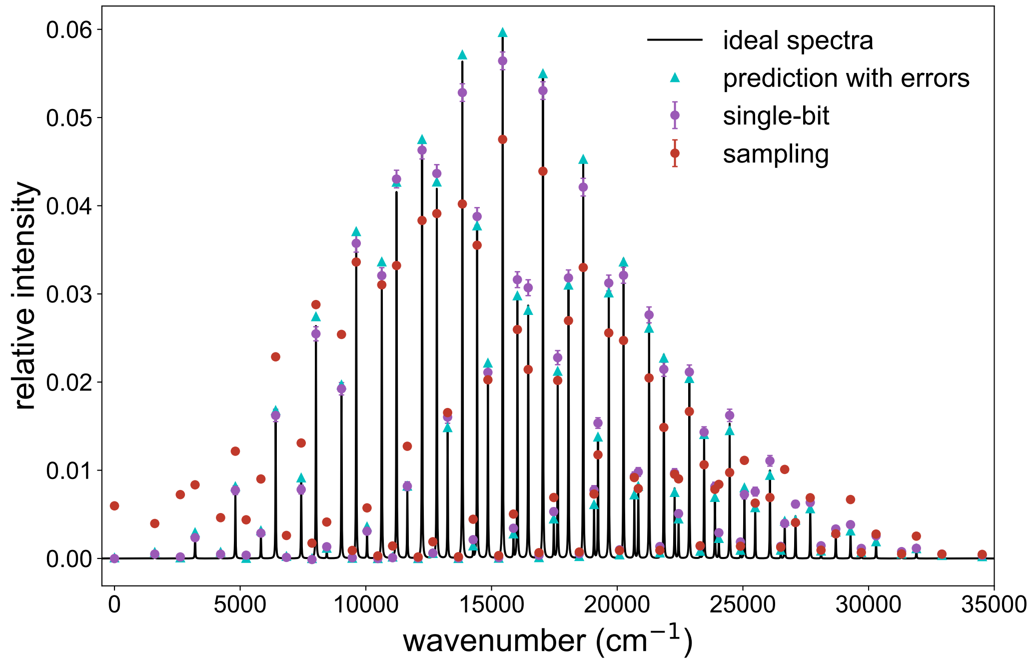

FIG. 1. Photoionization of neutral water to the ($\tilde{B}^2B_2$) excited state of the cation starting in the vibrationless state $n = 0$, $m = 0$.

	$H_2O \xrightarrow{h\nu} H_2O^+(\tilde{B}^2B_2) + e^-$ starting in ($n = 0$, $m = 0$)			
(n', m')	Classically calculated	Master equation simulation	Single-bit extraction	Sampling
(0,0)	7.92E-05	8.26E-05	0	0.006 ± 0.0001
(0,1)	6.67E-04	7.01E-04	0.0005 ± 0.0002	0.00396 ± 0.0001
(0,2)	2.80E-03	2.94E-03	0.0024 ± 0.0003	0.0084 ± 0.0001
(0,3)	7.76E-03	8.15E-03	0.0077 ± 0.0005	0.0122 ± 0.0002
(0,4)	1.60E-02	1.68E-02	0.0162 ± 0.0007	0.0229 ± 0.0002
(0,5)	2.64E-02	2.74E-02	0.0255 ± 0.0008	0.0288 ± 0.0003
(0,6)	3.59E-02	3.70E-02	0.0357 ± 0.001	0.0336 ± 0.0003
(0,7)	4.16E-02	4.26E-02	0.043 ± 0.001	0.0332 ± 0.0003
(0,8)	4.19E-02	4.27E-02	0.044 ± 0.001	0.0391 ± 0.0003
(0,9)	3.73E-02	3.77E-02	0.039 ± 0.001	0.0355 ± 0.0003
(0,10)	2.96E-02	2.98E-02	0.0316 ± 0.0009	0.026 ± 0.0003
(0,11)	2.13E-02	2.12E-02	0.0228 ± 0.0008	0.0202 ± 0.0002
(0,12)	1.39E-02	1.38E-02	0.0154 ± 0.0006	0.0118 ± 0.0002
(0,13)	8.33E-03	8.20E-03	0.0098 ± 0.0005	0.0079 ± 0.0001
(0,14)	4.60E-03	4.50E-03	0.0051 ± 0.0004	0.009 ± 0.0001
(0,15)	2.36E-03	2.29E-03	0.0029 ± 0.0003	0.0084 ± 0.0001
(1,0)	7.82E-05	8.11E-05	0.0002 ± 0.0002	0.0072 ± 0.0001
(1,1)	6.91E-04	7.19E-04	0.0005 ± 0.0002	0.0046 ± 0.0001
(1,2)	3.03E-03	3.16E-03	0.0029 ± 0.0003	0.009 ± 0.0001
(1,3)	8.81E-03	9.14E-03	0.0078 ± 0.0005	0.0131 ± 0.0002
(1,4)	1.91E-02	1.97E-02	0.0192 ± 0.0007	0.0254 ± 0.0002
(1,5)	3.28E-02	3.36E-02	0.0321 ± 0.0009	0.031 ± 0.0003
(1,6)	4.66E-02	4.75E-02	0.046 ± 0.001	0.0383 ± 0.0003
(1,7)	5.63E-02	5.71E-02	0.053 ± 0.001	0.0402 ± 0.0003
(1,8)	5.92E-02	5.97E-02	0.056 ± 0.001	0.0475 ± 0.0003
(1,9)	5.49E-02	5.50E-02	0.053 ± 0.001	0.0439 ± 0.0003

(1,10)	4.55E-02	4.53E-02	0.042 ± 0.001	0.033 ± 0.0003
(1,11)	3.40E-02	3.37E-02	0.0321 ± 0.0009	0.0247 ± 0.0002
(1,12)	2.32E-02	2.28E-02	0.0214 ± 0.0008	0.0149 ± 0.0002
(1,13)	1.44E-02	1.41E-02	0.0143 ± 0.0006	0.0106 ± 0.0002
(1,14)	8.30E-03	8.04E-03	0.0073 ± 0.0005	0.0111 ± 0.0002
(1,15)	4.42E-03	4.25E-03	0.004 ± 0.0004	0.0101 ± 0.0002
(2,0)	2.61E-05	2.68E-05	0.0004 ± 0.0001	0.0044 ± 0.0001
(2,1)	2.47E-04	2.52E-04	0.0001 ± 0.0001	0.00261 ± 8E-05
(2,2)	1.15E-03	1.17E-03	0.0013 ± 0.0002	0.0041 ± 0.0001
(2,3)	3.57E-03	3.60E-03	0.0031 ± 0.0003	0.0057 ± 0.0001
(2,4)	8.19E-03	8.21E-03	0.0082 ± 0.0005	0.0127 ± 0.0002
(2,5)	1.49E-02	1.48E-02	0.016 ± 0.0007	0.0165 ± 0.0002
(2,6)	2.25E-02	2.22E-02	0.0211 ± 0.0008	0.0203 ± 0.0002
(2,7)	2.87E-02	2.81E-02	0.0307 ± 0.0009	0.0214 ± 0.0002
(2,8)	3.19E-02	3.10E-02	0.0318 ± 0.0009	0.027 ± 0.0003
(2,9)	3.12E-02	3.01E-02	0.0312 ± 0.0009	0.0256 ± 0.0002
(2,10)	2.72E-02	2.61E-02	0.0276 ± 0.0009	0.0205 ± 0.0002
(2,11)	2.14E-02	2.04E-02	0.0211 ± 0.0008	0.0167 ± 0.0002
(2,12)	1.53E-02	1.45E-02	0.0162 ± 0.0007	0.0097 ± 0.0002
(2,13)	1.00E-02	9.46E-03	0.0111 ± 0.0006	0.0069 ± 0.0001
(2,14)	6.02E-03	5.67E-03	0.0064 ± 0.0004	0.0069 ± 0.0001
(2,15)	3.36E-03	3.14E-03	0.0038 ± 0.0003	0.0067 ± 0.0001
(3,0)	2.78E-06	3.35E-06	0	0.00174 ± 7E-05
(3,1)	2.97E-05	3.43E-05	8E-05 ± 8E-05	0.00091 ± 5E-05
(3,2)	1.56E-04	1.74E-04	9E-05 ± 8E-05	0.00142 ± 6E-05
(3,3)	5.37E-04	5.79E-04	0.0006 ± 0.0002	0.00189 ± 7E-05
(3,4)	1.36E-03	1.43E-03	0.0021 ± 0.0003	0.0044 ± 0.0001
(3,5)	2.73E-03	2.79E-03	0.0034 ± 0.0003	0.005 ± 0.0001
(3,6)	4.50E-03	4.49E-03	0.0053 ± 0.0004	0.0069 ± 0.0001
(3,7)	6.26E-03	6.12E-03	0.0078 ± 0.0005	0.0073 ± 0.0001
(3,8)	7.52E-03	7.22E-03	0.0093 ± 0.0005	0.0092 ± 0.0002
(3,9)	7.94E-03	7.50E-03	0.0097 ± 0.0005	0.0095 ± 0.0002
(3,10)	7.46E-03	6.94E-03	0.0082 ± 0.0005	0.0078 ± 0.0001
(3,11)	6.29E-03	5.78E-03	0.0076 ± 0.0005	0.0063 ± 0.0001
(3,12)	4.81E-03	4.37E-03	0.0062 ± 0.0004	0.0041 ± 0.0001
(3,13)	3.36E-03	3.01E-03	0.0033 ± 0.0003	0.00279 ± 8E-05
(3,14)	2.16E-03	1.91E-03	0.0026 ± 0.0003	0.00277 ± 8E-05
(3,15)	1.28E-03	1.12E-03	0.0012 ± 0.0002	0.00253 ± 8E-05
(4,0)	2.66E-09	1.53E-07	0	0.00029 ± 3E-05
(4,1)	1.45E-07	1.74E-06	6E-05 ± 5E-05	0.00017 ± 2E-05
(4,2)	1.73E-06	9.99E-06	6E-05 ± 6E-05	0.0002 ± 2E-05
(4,3)	1.02E-05	3.79E-05	0.0001 ± 8E-05	0.00033 ± 3E-05
(4,4)	3.86E-05	1.06E-04	0.0004 ± 0.0001	0.00065 ± 4E-05
(4,5)	1.06E-04	2.33E-04	0.0005 ± 0.0002	0.00073 ± 4E-05
(4,6)	2.25E-04	4.19E-04	0.001 ± 0.0002	0.0009 ± 5E-05
(4,7)	3.88E-04	6.34E-04	0.0014 ± 0.0002	0.00092 ± 5E-05
(4,8)	5.63E-04	8.24E-04	0.0014 ± 0.0002	0.00144 ± 6E-05
(4,9)	7.01E-04	9.36E-04	0.0019 ± 0.0003	0.00139 ± 6E-05
(4,10)	7.63E-04	9.43E-04	0.0014 ± 0.0002	0.00127 ± 6E-05
(4,11)	7.36E-04	8.50E-04	0.0014 ± 0.0002	0.00094 ± 5E-05
(4,12)	6.36E-04	6.92E-04	0.0011 ± 0.0002	0.00067 ± 4E-05
(4,13)	4.97E-04	5.13E-04	0.0008 ± 0.0002	0.00051 ± 4E-05
(4,14)	3.54E-04	3.49E-04	0.0005 ± 0.0001	0.00049 ± 3E-05
(4,15)	2.31E-04	2.18E-04	0.0004 ± 0.0001	0.00046 ± 3E-05

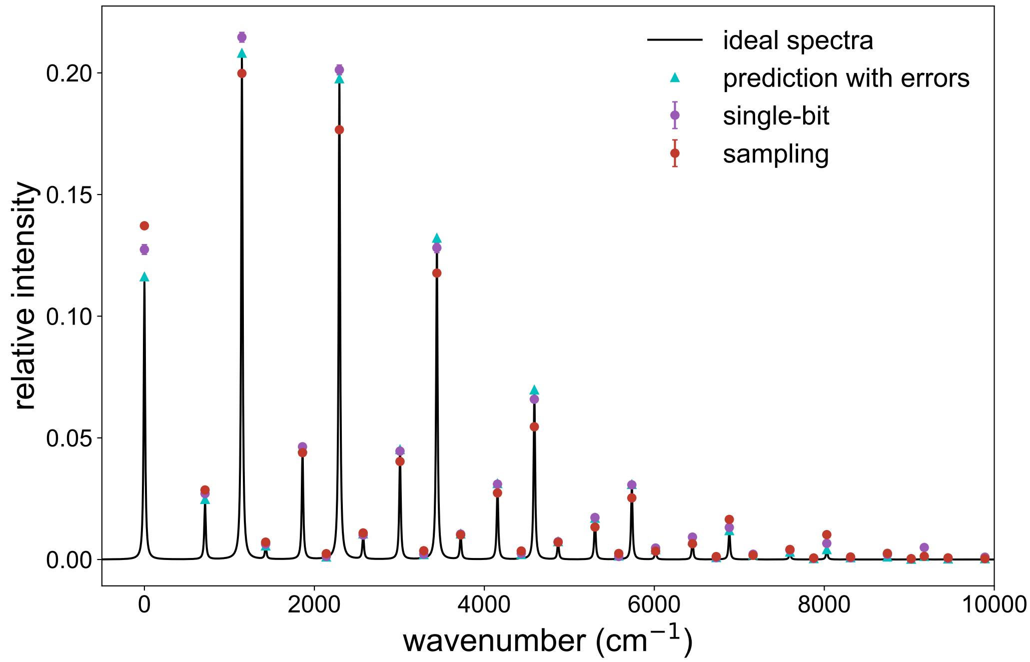

FIG. 2. Photoionization of the ozone anion to neutral ozone starting in the vibrationless state $n = 0$, $m = 0$.

	$O_3^- \xrightarrow{h\nu} O_3 + e^-$ starting in $(n = 0, m = 0)$			
(n', m')	Classically calculated	Master equation simulation	Single-bit extraction	Sampling
(0,0)	1.14E-01	1.16E-01	0.127 ± 0.002	0.1372 ± 0.0005
(0,1)	2.42E-02	2.47E-02	0.0271 ± 0.0008	0.0286 ± 0.0003
(0,2)	5.57E-03	5.60E-03	0.0063 ± 0.0004	0.0071 ± 0.0001
(0,3)	1.06E-03	1.06E-03	0.0013 ± 0.0002	0.0024 ± 8E-05
(1,0)	2.06E-01	2.08E-01	0.215 ± 0.002	0.1998 ± 0.0006
(1,1)	4.55E-02	4.60E-02	0.046 ± 0.001	0.0439 ± 0.0003
(1,2)	1.06E-02	1.06E-02	0.01 ± 0.0005	0.0109 ± 0.0002
(1,3)	2.06E-03	2.04E-03	0.0022 ± 0.0003	0.0036 ± 0.0001
(2,0)	1.98E-01	1.98E-01	0.201 ± 0.002	0.1766 ± 0.0006
(2,1)	4.52E-02	4.52E-02	0.045 ± 0.001	0.0403 ± 0.0003
(2,2)	1.07E-02	1.05E-02	0.0104 ± 0.0005	0.0101 ± 0.0002
(2,3)	2.11E-03	2.06E-03	0.0025 ± 0.0003	0.00349 ± 9E-05
(3,0)	1.33E-01	1.32E-01	0.128 ± 0.002	0.1177 ± 0.0005
(3,1)	3.15E-02	3.12E-02	0.031 ± 0.0009	0.0274 ± 0.0003
(3,2)	7.54E-03	7.37E-03	0.0073 ± 0.0005	0.0071 ± 0.0001
(3,3)	1.51E-03	1.47E-03	0.0012 ± 0.0002	0.00248 ± 8E-05
(4,0)	7.08E-02	6.97E-02	0.066 ± 0.001	0.0546 ± 0.0004
(4,1)	1.73E-02	1.70E-02	0.0173 ± 0.0007	0.0133 ± 0.0002
(4,2)	4.19E-03	4.06E-03	0.0047 ± 0.0004	0.00342 ± 9E-05
(4,3)	8.51E-04	8.19E-04	0.0008 ± 0.0002	0.0012 ± 6E-05
(5,0)	3.15E-02	3.09E-02	0.0307 ± 0.0009	0.0253 ± 0.0003
(5,1)	7.91E-03	7.74E-03	0.0092 ± 0.0005	0.0065 ± 0.0001
(5,2)	1.94E-03	1.87E-03	0.0022 ± 0.0003	0.00173 ± 7E-05
(5,3)	4.01E-04	3.83E-04	0.0004 ± 0.0001	0.00064 ± 4E-05
(6,0)	1.22E-02	1.19E-02	0.0132 ± 0.0007	0.0165 ± 0.0002
(6,1)	3.15E-03	3.07E-03	0.0039 ± 0.0004	0.0041 ± 0.0001
(6,2)	7.83E-04	7.52E-04	0.0007 ± 0.0002	0.00105 ± 5E-05

(6,3)	1.64E-04	1.56E-04	0.00024 ± 9E-05	0.00036 ± 3E-05
(7,0)	4.23E-03	4.10E-03	0.0066 ± 0.0005	0.0102 ± 0.0002
(7,1)	1.12E-03	1.09E-03	0.0021 ± 0.0003	0.00252 ± 8E-05
(7,2)	2.81E-04	2.69E-04	0.0005 ± 0.0001	0.00068 ± 4E-05
(7,3)	5.96E-05	5.64E-05	0.00019 ± 8E-05	0.00017 ± 2E-05
(8,0)	1.33E-03	1.28E-03	0.0049 ± 0.0005	0.00132 ± 6E-05
(8,1)	3.61E-04	3.48E-04	0.001 ± 0.0002	0.00035 ± 3E-05
(8,2)	9.18E-05	8.73E-05	0.0002 ± 0.0001	9E-05 ± 2E-05
(8,3)	1.97E-05	1.85E-05	0.00013 ± 7E-05	2.8E-05 ± 8E-06
(9,0)	3.86E-04	3.68E-04	0.0047 ± 0.0005	0.00156 ± 6E-05
(9,1)	1.07E-04	1.03E-04	0.0012 ± 0.0002	0.00038 ± 3E-05
(9,2)	2.76E-05	2.60E-05	0.0004 ± 0.0001	8E-05 ± 1E-05
(9,3)	5.98E-06	5.59E-06	0.00013 ± 7E-05	3.6E-05 ± 1E-05

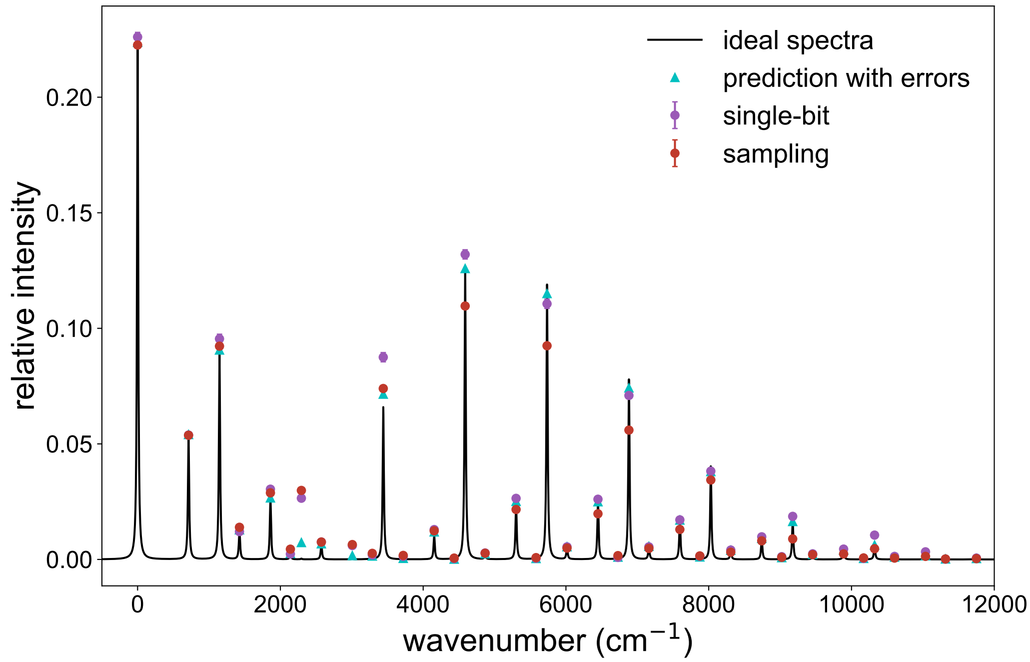

FIG. 3. Photoionization of the ozone anion to neutral ozone starting with one quanta in the symmetric-stretching mode and zero in the bending mode $n = 1$, $m = 0$.

	$O_3^- \xrightarrow{h\nu} O_3 + e^-$ starting in $(n = 1, m = 0)$			
(n', m')	Classically calculated	Master equation simulation	Single-bit extraction	Sampling
(0,0)	2.24E-01	2.23E-01	0.226 ± 0.002	0.2226 ± 0.0007
(0,1)	5.42E-02	5.40E-02	0.054 ± 0.001	0.0537 ± 0.0004
(0,2)	1.31E-02	1.28E-02	0.0121 ± 0.0006	0.0139 ± 0.0002
(0,3)	2.64E-03	2.56E-03	0.0023 ± 0.0003	0.0044 ± 0.0001
(1,0)	8.96E-02	9.09E-02	0.095 ± 0.002	0.0923 ± 0.0005
(1,1)	2.67E-02	2.69E-02	0.0304 ± 0.0009	0.0288 ± 0.0003
(1,2)	6.90E-03	6.83E-03	0.0075 ± 0.0005	0.0075 ± 0.0001
(1,3)	1.51E-03	1.48E-03	0.002 ± 0.0003	0.00263 ± 9E-05
(2,0)	3.14E-04	5.76E-03	0.0265 ± 0.0009	0.0299 ± 0.0003
(2,1)	2.69E-04	1.39E-03	0.006 ± 0.0004	0.0064 ± 0.0001
(2,2)	1.59E-04	4.07E-04	0.0013 ± 0.0002	0.00174 ± 7E-05
(2,3)	6.61E-05	1.11E-04	0.0004 ± 0.0001	0.00059 ± 4E-05
(3,0)	6.59E-02	6.96E-02	0.088 ± 0.002	0.074 ± 0.0004
(3,1)	1.05E-02	1.14E-02	0.0129 ± 0.0006	0.0124 ± 0.0002
(3,2)	2.11E-03	2.27E-03	0.0028 ± 0.0003	0.00267 ± 9E-05
(3,3)	3.34E-04	3.67E-04	0.0005 ± 0.0001	0.00078 ± 5E-05
(4,0)	1.26E-01	1.25E-01	0.132 ± 0.002	0.1097 ± 0.0005
(4,1)	2.51E-02	2.49E-02	0.0264 ± 0.0009	0.0216 ± 0.0002
(4,2)	5.55E-03	5.42E-03	0.0054 ± 0.0004	0.0049 ± 0.0001
(4,3)	1.01E-03	9.81E-04	0.0009 ± 0.0002	0.00165 ± 7E-05
(5,0)	1.19E-01	1.16E-01	0.111 ± 0.002	0.0925 ± 0.0005
(5,1)	2.58E-02	2.51E-02	0.0261 ± 0.0009	0.0198 ± 0.0002
(5,2)	5.94E-03	5.68E-03	0.0054 ± 0.0004	0.0048 ± 0.0001
(5,3)	1.14E-03	1.08E-03	0.0014 ± 0.0002	0.00153 ± 7E-05
(6,0)	7.79E-02	7.54E-02	0.071 ± 0.001	0.056 ± 0.0004
(6,1)	1.79E-02	1.73E-02	0.0171 ± 0.0007	0.013 ± 0.0002

(6,2)	4.23E-03	4.01E-03	0.0041 ± 0.0004	0.00313 ± 9E-05
(6,3)	8.33E-04	7.82E-04	0.0012 ± 0.0002	0.00091 ± 5E-05
(7,0)	4.03E-02	3.89E-02	0.038 ± 0.001	0.0344 ± 0.0003
(7,1)	9.69E-03	9.34E-03	0.0098 ± 0.0005	0.008 ± 0.0001
(7,2)	2.33E-03	2.21E-03	0.0024 ± 0.0003	0.00207 ± 8E-05
(7,3)	4.70E-04	4.40E-04	0.0004 ± 0.0001	0.00065 ± 4E-05
(8,0)	1.75E-02	1.69E-02	0.0186 ± 0.0008	0.0089 ± 0.0002
(8,1)	4.38E-03	4.22E-03	0.0045 ± 0.0004	0.00239 ± 8E-05
(8,2)	1.07E-03	1.02E-03	0.0013 ± 0.0002	0.00059 ± 4E-05
(8,3)	2.20E-04	2.06E-04	0.00016 ± 8E-05	0.0002 ± 2E-05
(9,0)	6.66E-03	6.43E-03	0.0105 ± 0.0006	0.0046 ± 0.0001
(9,1)	1.72E-03	1.66E-03	0.0033 ± 0.0003	0.00132 ± 6E-05
(9,2)	4.28E-04	4.05E-04	0.0006 ± 0.0002	0.00034 ± 3E-05
(9,3)	8.93E-05	8.37E-05	3E-05 ± 6E-05	0.00013 ± 2E-05

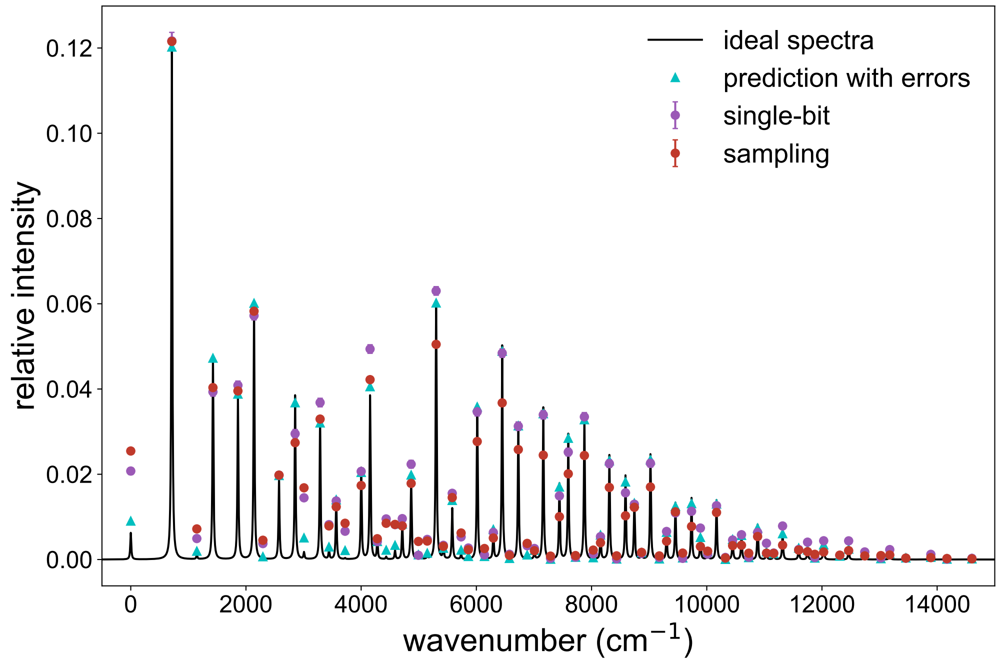

FIG. 4. Photoionization of the ozone anion to neutral ozone starting with one quanta in the symmetric-stretching mode and two in the bending mode $n = 1$, $m = 2$.

	$O_3^- \xrightarrow{h\nu} O_3 + e^-$ starting in ($n = 1$, $m = 2$)			
(n', m')	Classically calculated	Master equation simulation	Single-bit extraction	Sampling
(0,0)	6.24E-03	9.10E-03	0.0208 ± 0.0008	0.0255 ± 0.0003
(0,1)	1.21E-01	1.20E-01	0.122 ± 0.002	0.1215 ± 0.0006
(0,2)	4.73E-02	4.75E-02	0.039 ± 0.001	0.0403 ± 0.0004
(0,3)	6.01E-02	6.02E-02	0.057 ± 0.001	0.0583 ± 0.0004
(0,4)	3.85E-02	3.65E-02	0.0295 ± 0.001	0.0274 ± 0.0003
(0,5)	1.46E-02	1.39E-02	0.0137 ± 0.0007	0.0124 ± 0.0002
(0,6)	4.57E-03	4.18E-03	0.0042 ± 0.0004	0.0049 ± 0.0001
(0,7)	1.21E-03	1.10E-03	0.001 ± 0.0002	0.0042 ± 0.0001
(1,0)	9.99E-04	1.99E-03	0.0049 ± 0.0004	0.0072 ± 0.0002
(1,1)	3.79E-02	3.89E-02	0.041 ± 0.001	0.0395 ± 0.0004
(1,2)	1.90E-02	1.99E-02	0.0198 ± 0.0008	0.0198 ± 0.0003
(1,3)	3.22E-02	3.22E-02	0.037 ± 0.001	0.0329 ± 0.0003
(1,4)	2.14E-02	2.04E-02	0.0207 ± 0.0008	0.0174 ± 0.0002
(1,5)	8.78E-03	8.31E-03	0.0096 ± 0.0006	0.0079 ± 0.0002
(1,6)	2.87E-03	2.63E-03	0.0033 ± 0.0003	0.0031 ± 0.0001
(1,7)	7.99E-04	7.23E-04	0.0011 ± 0.0002	0.00258 ± 0.0001
(2,0)	4.14E-04	6.10E-04	0.0037 ± 0.0004	0.0045 ± 0.0001
(2,1)	1.56E-03	4.26E-03	0.0145 ± 0.0007	0.0168 ± 0.0002
(2,2)	2.44E-04	1.72E-03	0.0066 ± 0.0005	0.0085 ± 0.0002
(2,3)	5.64E-04	1.90E-03	0.0095 ± 0.0006	0.0085 ± 0.0002
(2,4)	6.09E-04	1.33E-03	0.0047 ± 0.0004	0.0043 ± 0.0001
(2,5)	4.53E-04	6.66E-04	0.0027 ± 0.0003	0.00229 ± 9E-05
(2,6)	1.95E-04	2.51E-04	0.0012 ± 0.0002	0.00098 ± 6E-05
(2,7)	6.97E-05	7.85E-05	0.0003 ± 0.0001	0.0008 ± 5E-05
(3,0)	2.02E-03	2.95E-03	0.0082 ± 0.0005	0.0079 ± 0.0002
(3,1)	3.84E-02	3.97E-02	0.049 ± 0.001	0.0422 ± 0.0004

(3,2)	1.87E-02	1.94E-02	0.0224 ± 0.0009	0.0179 ± 0.0003
(3,3)	1.20E-02	1.34E-02	0.0155 ± 0.0007	0.0145 ± 0.0002
(3,4)	6.36E-03	6.72E-03	0.0064 ± 0.0005	0.0051 ± 0.0001
(3,5)	1.83E-03	2.05E-03	0.0026 ± 0.0003	0.00206 ± 9E-05
(3,6)	4.70E-04	5.06E-04	0.0006 ± 0.0002	0.00093 ± 6E-05
(3,7)	9.93E-05	1.14E-04	0.0002 ± 0.0001	0.00086 ± 6E-05
(4,0)	2.05E-03	3.41E-03	0.0082 ± 0.0005	0.0082 ± 0.0002
(4,1)	6.06E-02	6.01E-02	0.063 ± 0.001	0.0505 ± 0.0004
(4,2)	3.64E-02	3.58E-02	0.035 ± 0.001	0.0277 ± 0.0003
(4,3)	3.11E-02	3.13E-02	0.031 ± 0.001	0.0258 ± 0.0003
(4,4)	1.77E-02	1.68E-02	0.0149 ± 0.0007	0.01 ± 0.0002
(4,5)	5.91E-03	5.69E-03	0.0054 ± 0.0004	0.0039 ± 0.0001
(4,6)	1.69E-03	1.55E-03	0.0014 ± 0.0002	0.00167 ± 8E-05
(4,7)	4.09E-04	3.80E-04	0.0003 ± 0.0001	0.00151 ± 7E-05
(5,0)	1.18E-03	2.29E-03	0.0053 ± 0.0004	0.0062 ± 0.0002
(5,1)	5.02E-02	4.93E-02	0.048 ± 0.001	0.0367 ± 0.0004
(5,2)	3.57E-02	3.46E-02	0.034 ± 0.001	0.0245 ± 0.0003
(5,3)	3.39E-02	3.31E-02	0.033 ± 0.001	0.0244 ± 0.0003
(5,4)	1.96E-02	1.82E-02	0.0156 ± 0.0007	0.0103 ± 0.0002
(5,5)	6.87E-03	6.40E-03	0.0066 ± 0.0005	0.0043 ± 0.0001
(5,6)	2.03E-03	1.81E-03	0.0012 ± 0.0002	0.00196 ± 8E-05
(5,7)	5.10E-04	4.57E-04	0.0005 ± 0.0002	0.00148 ± 7E-05
(6,0)	4.73E-04	1.13E-03	0.0032 ± 0.0003	0.0038 ± 0.0001
(6,1)	2.94E-02	2.89E-02	0.0252 ± 0.0009	0.0201 ± 0.0003
(6,2)	2.45E-02	2.36E-02	0.0225 ± 0.0009	0.0169 ± 0.0002
(6,3)	2.47E-02	2.37E-02	0.0226 ± 0.0009	0.017 ± 0.0002
(6,4)	1.44E-02	1.32E-02	0.0113 ± 0.0006	0.0078 ± 0.0002
(6,5)	5.18E-03	4.76E-03	0.0046 ± 0.0004	0.0033 ± 0.0001
(6,6)	1.56E-03	1.38E-03	0.0015 ± 0.0002	0.00143 ± 7E-05
(6,7)	4.00E-04	3.53E-04	0.0005 ± 0.0001	0.00122 ± 7E-05
(7,0)	1.44E-04	4.53E-04	0.0013 ± 0.0002	0.00221 ± 9E-05
(7,1)	1.37E-02	1.35E-02	0.013 ± 0.0007	0.0122 ± 0.0002
(7,2)	1.33E-02	1.28E-02	0.0109 ± 0.0006	0.0112 ± 0.0002
(7,3)	1.39E-02	1.33E-02	0.0126 ± 0.0007	0.011 ± 0.0002
(7,4)	8.18E-03	7.46E-03	0.0064 ± 0.0005	0.0054 ± 0.0001
(7,5)	3.00E-03	2.73E-03	0.0024 ± 0.0003	0.00221 ± 9E-05
(7,6)	9.14E-04	8.02E-04	0.001 ± 0.0002	0.00102 ± 6E-05
(7,7)	2.38E-04	2.08E-04	0.0004 ± 0.0001	0.00092 ± 6E-05
(8,0)	3.37E-05	1.55E-04	0.0005 ± 0.0002	0.00085 ± 6E-05
(8,1)	5.37E-03	5.35E-03	0.0074 ± 0.0005	0.003 ± 0.0001
(8,2)	6.07E-03	5.83E-03	0.0058 ± 0.0005	0.0033 ± 0.0001
(8,3)	6.54E-03	6.22E-03	0.0079 ± 0.0005	0.0034 ± 0.0001
(8,4)	3.86E-03	3.52E-03	0.0044 ± 0.0004	0.00176 ± 8E-05
(8,5)	1.44E-03	1.30E-03	0.0018 ± 0.0003	0.00085 ± 6E-05
(8,6)	4.42E-04	3.88E-04	0.0003 ± 0.0001	0.00033 ± 3E-05
(8,7)	1.17E-04	1.02E-04	0.0001 ± 7E-05	0.00023 ± 3E-05
(9,0)	5.90E-06	4.75E-05	0.0005 ± 0.0002	0.00035 ± 4E-05
(9,1)	1.84E-03	1.84E-03	0.0038 ± 0.0004	0.00149 ± 7E-05
(9,2)	2.42E-03	2.32E-03	0.0041 ± 0.0004	0.00184 ± 8E-05
(9,3)	2.67E-03	2.53E-03	0.0044 ± 0.0004	0.00208 ± 9E-05
(9,4)	1.58E-03	1.44E-03	0.0023 ± 0.0003	0.00105 ± 6E-05
(9,5)	5.95E-04	5.39E-04	0.0012 ± 0.0002	0.00044 ± 4E-05
(9,6)	1.85E-04	1.62E-04	0.0003 ± 0.0001	0.00016 ± 2E-05
(9,7)	4.94E-05	4.28E-05	0.00012 ± 7E-05	0.00015 ± 2E-05

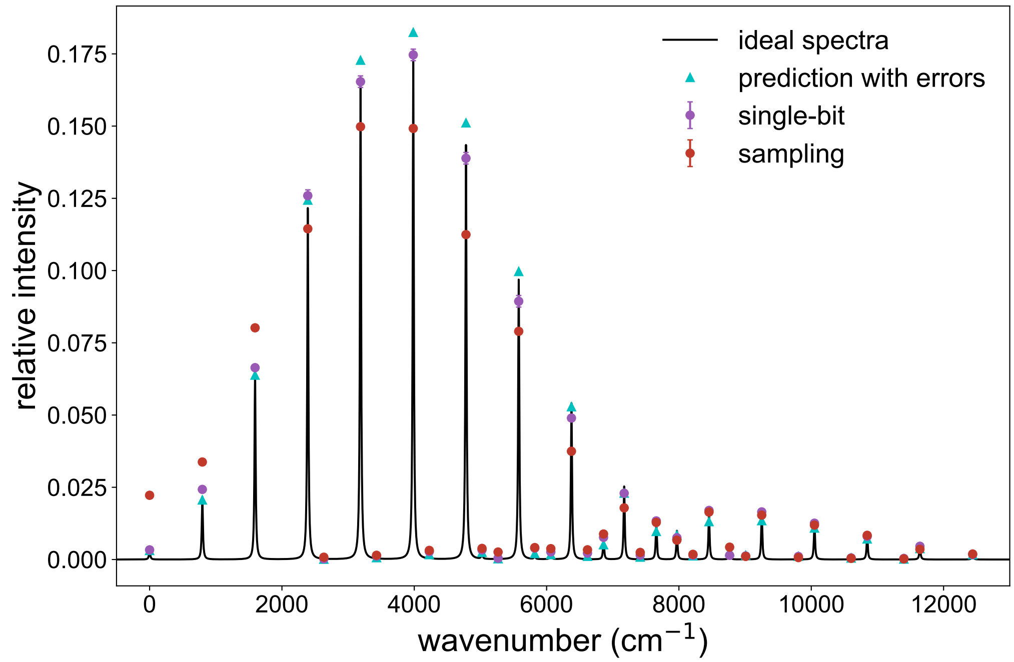

FIG. 5. Photoionization of nitrite to nitrogen dioxide starting in the vibrationless state $n = 0$, $m = 0$.

	$NO_2^- \xrightarrow{h\nu} NO_2 + e^-$ starting in $(n = 0, m = 0)$			
(n', m')	Classically calculated	Master equation simulation	Single-bit extraction	Sampling
(0,0)	3.54E-03	3.14E-03	0.0033 ± 0.0004	0.0222 ± 0.0002
(0,1)	2.17E-02	2.07E-02	0.0243 ± 0.0008	0.0337 ± 0.0003
(0,2)	6.42E-02	6.40E-02	0.066 ± 0.001	0.0802 ± 0.0004
(0,3)	1.22E-01	1.24E-01	0.126 ± 0.002	0.1145 ± 0.0005
(0,4)	1.66E-01	1.73E-01	0.165 ± 0.002	0.1498 ± 0.0006
(0,5)	1.73E-01	1.82E-01	0.175 ± 0.002	0.1492 ± 0.0005
(0,6)	1.43E-01	1.51E-01	0.139 ± 0.002	0.1125 ± 0.0005
(0,7)	9.68E-02	9.95E-02	0.089 ± 0.002	0.079 ± 0.0004
(0,8)	5.41E-02	5.27E-02	0.049 ± 0.001	0.0375 ± 0.0003
(0,9)	2.53E-02	2.29E-02	0.0229 ± 0.0008	0.0179 ± 0.0002
(0,10)	9.93E-03	8.49E-03	0.0076 ± 0.0005	0.0067 ± 0.0001
(0,11)	3.29E-03	2.75E-03	0.0014 ± 0.0003	0.0043 ± 0.0001
(1,0)	2.74E-04	1.03E-04	0.00026 ± 0.0001	0.0008 ± 4E-05
(1,1)	1.18E-03	6.52E-04	0.0012 ± 0.0002	0.00147 ± 6E-05
(1,2)	2.24E-03	1.73E-03	0.0027 ± 0.0003	0.00316 ± 9E-05
(1,3)	2.32E-03	2.48E-03	0.0033 ± 0.0003	0.00384 ± 0.0001
(1,4)	1.26E-03	2.04E-03	0.0039 ± 0.0004	0.00414 ± 0.0001
(1,5)	2.02E-04	1.04E-03	0.0022 ± 0.0003	0.00336 ± 9E-05
(1,6)	6.79E-05	7.77E-04	0.0015 ± 0.0002	0.00245 ± 8E-05
(1,7)	6.34E-04	1.27E-03	0.0015 ± 0.0002	0.0018 ± 7E-05
(1,8)	1.12E-03	1.53E-03	0.0012 ± 0.0002	0.00107 ± 5E-05
(1,9)	1.13E-03	1.15E-03	0.0011 ± 0.0002	0.00067 ± 4E-05
(1,10)	8.04E-04	5.44E-04	0.0005 ± 0.0001	0.00039 ± 3E-05
(1,11)	4.38E-04	1.56E-04	0.0004 ± 0.0001	0.00021 ± 2E-05
(2,0)	4.71E-04	2.67E-04	0.0005 ± 0.0001	0.0026 ± 8E-05
(2,1)	2.62E-03	1.71E-03	0.0026 ± 0.0003	0.00376 ± 9E-05
(2,2)	7.06E-03	5.16E-03	0.0077 ± 0.0005	0.0088 ± 0.0001

(2,3)	1.24E-02	9.77E-03	0.0134 ± 0.0006	0.0128 ± 0.0002
(2,4)	1.58E-02	1.31E-02	0.017 ± 0.0007	0.0164 ± 0.0002
(2,5)	1.58E-02	1.35E-02	0.0165 ± 0.0007	0.0154 ± 0.0002
(2,6)	1.28E-02	1.09E-02	0.0126 ± 0.0006	0.0119 ± 0.0002
(2,7)	8.70E-03	7.12E-03	0.008 ± 0.0005	0.0084 ± 0.0001
(2,8)	5.07E-03	3.79E-03	0.0046 ± 0.0004	0.00354 ± 9E-05
(2,9)	2.56E-03	1.67E-03	0.0017 ± 0.0002	0.00191 ± 7E-05
(2,10)	1.14E-03	6.20E-04	0.0008 ± 0.0002	0.00064 ± 4E-05
(2,11)	4.45E-04	1.96E-04	0.0005 ± 0.0001	0.00039 ± 3E-05

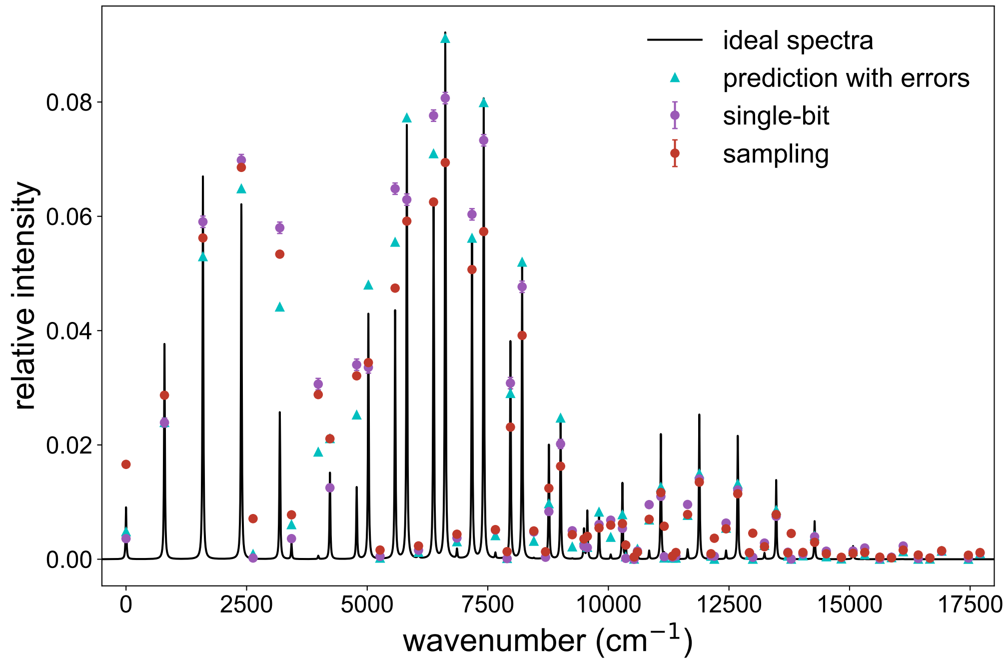

FIG. 6. Photoionization of nitrite to nitrogen dioxide starting with one quanta in the symmetric-stretching mode and zero in the bending mode $n = 1$, $m = 0$. The more significant errors are primarily due to having a large self-Kerr on cavity A (∼30 kHz) during the beamsplitter operation after starting in a state with higher photon number.

	$NO_2^- \xrightarrow{h\nu} NO_2 + e^-$ starting in $(n = 1,\ m = 0)$			
(n', m')	Classically calculated	Master equation simulation	Single-bit extraction	Sampling
(0,0)	9.08E-03	4.87E-03	0.0036 ± 0.0004	0.0166 ± 0.0002
(0,1)	3.77E-02	2.40E-02	0.0239 ± 0.0008	0.0287 ± 0.0003
(0,2)	6.70E-02	5.28E-02	0.059 ± 0.001	0.0562 ± 0.0004
(0,3)	6.21E-02	6.36E-02	0.07 ± 0.001	0.0686 ± 0.0004
(0,4)	2.57E-02	4.12E-02	0.058 ± 0.001	0.0534 ± 0.0004
(0,5)	5.78E-04	1.47E-02	0.0306 ± 0.001	0.0288 ± 0.0003
(0,6)	1.25E-02	2.20E-02	0.034 ± 0.001	0.0321 ± 0.0003
(0,7)	4.34E-02	5.43E-02	0.065 ± 0.001	0.0474 ± 0.0004
(0,8)	6.17E-02	7.15E-02	0.078 ± 0.001	0.0625 ± 0.0004
(0,9)	5.65E-02	5.71E-02	0.06 ± 0.001	0.0507 ± 0.0004
(0,10)	3.80E-02	2.95E-02	0.0308 ± 0.001	0.0231 ± 0.0003
(0,11)	2.00E-02	9.85E-03	0.0083 ± 0.0005	0.0124 ± 0.0002
(0,12)	8.41E-03	2.11E-03	0.002 ± 0.0003	0.004 ± 0.0001
(0,13)	2.87E-03	4.62E-04	0.0002 ± 0.0002	0.00248 ± 9E-05
(0,14)	8.00E-04	2.41E-04	0.0004 ± 0.0002	0.0058 ± 0.0001
(1,0)	1.46E-04	9.10E-04	0.0002 ± 0.0002	0.0071 ± 0.0001
(1,1)	2.73E-03	6.17E-03	0.0036 ± 0.0004	0.0078 ± 0.0002
(1,2)	1.51E-02	2.15E-02	0.0125 ± 0.0006	0.0211 ± 0.0002
(1,3)	4.29E-02	4.89E-02	0.0336 ± 0.001	0.0344 ± 0.0003
(1,4)	7.59E-02	7.90E-02	0.063 ± 0.001	0.0592 ± 0.0004
(1,5)	9.21E-02	9.34E-02	0.081 ± 0.001	0.0694 ± 0.0004
(1,6)	8.05E-02	8.20E-02	0.073 ± 0.001	0.0573 ± 0.0004
(1,7)	5.16E-02	5.33E-02	0.048 ± 0.001	0.0392 ± 0.0003
(1,8)	2.39E-02	2.52E-02	0.0202 ± 0.0008	0.0163 ± 0.0002

(1,9)	7.45E-03	8.37E-03	0.0061 ± 0.0005	0.0055 ± 0.0001
(1,10)	1.24E-03	1.78E-03	0.0014 ± 0.0003	0.00124 ± 6E-05
(1,11)	1.95E-05	1.99E-04	0.0006 ± 0.0002	0.00118 ± 6E-05
(1,12)	8.94E-05	1.33E-05	0.0005 ± 0.0002	0.0037 ± 0.0001
(1,13)	1.56E-04	1.69E-05	0.0003 ± 0.0002	0.0046 ± 0.0001
(1,14)	1.08E-04	2.40E-05	0	0.0045 ± 0.0001
(2,0)	3.83E-04	1.99E-04	0.0005 ± 0.0001	0.00161 ± 7E-05
(2,1)	1.23E-03	1.20E-03	0.0016 ± 0.0002	0.00233 ± 8E-05
(2,2)	1.61E-03	3.06E-03	0.0037 ± 0.0004	0.0044 ± 0.0001
(2,3)	9.74E-04	4.06E-03	0.0051 ± 0.0004	0.0052 ± 0.0001
(2,4)	1.41E-04	2.92E-03	0.0048 ± 0.0004	0.005 ± 0.0001
(2,5)	1.05E-04	1.84E-03	0.005 ± 0.0004	0.0043 ± 0.0001
(2,6)	7.93E-04	3.63E-03	0.0068 ± 0.0005	0.006 ± 0.0001
(2,7)	1.49E-03	6.90E-03	0.0096 ± 0.0005	0.007 ± 0.0001
(2,8)	1.71E-03	7.86E-03	0.0096 ± 0.0005	0.0078 ± 0.0002
(2,9)	1.50E-03	5.59E-03	0.0063 ± 0.0004	0.0053 ± 0.0001
(2,10)	1.08E-03	2.48E-03	0.0028 ± 0.0003	0.00219 ± 8E-05
(2,11)	6.70E-04	6.10E-04	0.0009 ± 0.0002	0.0012 ± 6E-05
(2,12)	3.63E-04	5.24E-05	0.0003 ± 0.0001	0.00034 ± 3E-05
(2,13)	1.72E-04	1.32E-05	0.0001 ± 8E-05	0.00037 ± 3E-05
(2,14)	7.12E-05	2.40E-05	0.00014 ± 9E-05	0.00074 ± 5E-05
(3,0)	8.70E-05	1.50E-04	0.00012 ± 9E-05	0.00133 ± 6E-05
(3,1)	1.12E-03	9.95E-04	0.0003 ± 0.0001	0.00132 ± 6E-05
(3,2)	5.23E-03	3.46E-03	0.0023 ± 0.0003	0.0036 ± 0.0001
(3,3)	1.33E-02	7.92E-03	0.0054 ± 0.0004	0.0062 ± 0.0001
(3,4)	2.19E-02	1.29E-02	0.011 ± 0.0006	0.0117 ± 0.0002
(3,5)	2.53E-02	1.53E-02	0.014 ± 0.0007	0.0135 ± 0.0002
(3,6)	2.16E-02	1.35E-02	0.0121 ± 0.0006	0.0115 ± 0.0002
(3,7)	1.39E-02	8.77E-03	0.0075 ± 0.0005	0.0078 ± 0.0002
(3,8)	6.67E-03	4.15E-03	0.0039 ± 0.0004	0.00296 ± 9E-05
(3,9)	2.31E-03	1.37E-03	0.0014 ± 0.0002	0.00103 ± 6E-05
(3,10)	5.13E-04	2.86E-04	0.0004 ± 0.0001	0.00025 ± 3E-05
(3,11)	4.40E-05	3.18E-05	0.0002 ± 0.0001	0.00021 ± 2E-05
(3,12)	2.11E-06	7.28E-06	0.0002 ± 0.0001	0.00071 ± 5E-05
(3,13)	1.79E-05	8.77E-06	0.00018 ± 9E-05	0.00091 ± 5E-05
(3,14)	1.77E-05	7.78E-06	0.0001 ± 8E-05	0.00084 ± 5E-05
(4,0)	9.46E-06	3.58E-05	0	0.0004 ± 3E-05
(4,1)	8.74E-06	2.20E-04	0.0004 ± 0.0001	0.00055 ± 4E-05
(4,2)	2.89E-07	5.52E-04	0.0006 ± 0.0002	0.00096 ± 5E-05
(4,3)	3.10E-05	7.20E-04	0.0011 ± 0.0002	0.00115 ± 6E-05
(4,4)	8.57E-05	5.26E-04	0.0012 ± 0.0002	0.00112 ± 6E-05
(4,5)	9.82E-05	3.86E-04	0.0014 ± 0.0002	0.00095 ± 5E-05
(4,6)	6.28E-05	7.62E-04	0.002 ± 0.0003	0.00118 ± 6E-05
(4,7)	2.51E-05	1.35E-03	0.0023 ± 0.0003	0.0016 ± 7E-05
(4,8)	7.91E-06	1.48E-03	0.0014 ± 0.0002	0.00149 ± 7E-05
(4,9)	3.98E-06	1.03E-03	0.0011 ± 0.0002	0.00117 ± 6E-05
(4,10)	5.12E-06	4.58E-04	0.0004 ± 0.0001	0.00043 ± 4E-05
(4,11)	8.37E-06	1.20E-04	0.00015 ± 8E-05	0.00027 ± 3E-05
(4,12)	1.07E-05	1.67E-05	0	0.0001 ± 2E-05
(4,13)	1.00E-05	5.98E-06	0	7E-05 ± 1E-05
(4,14)	7.02E-06	5.32E-06	0.00015 ± 7E-05	0.00013 ± 2E-05

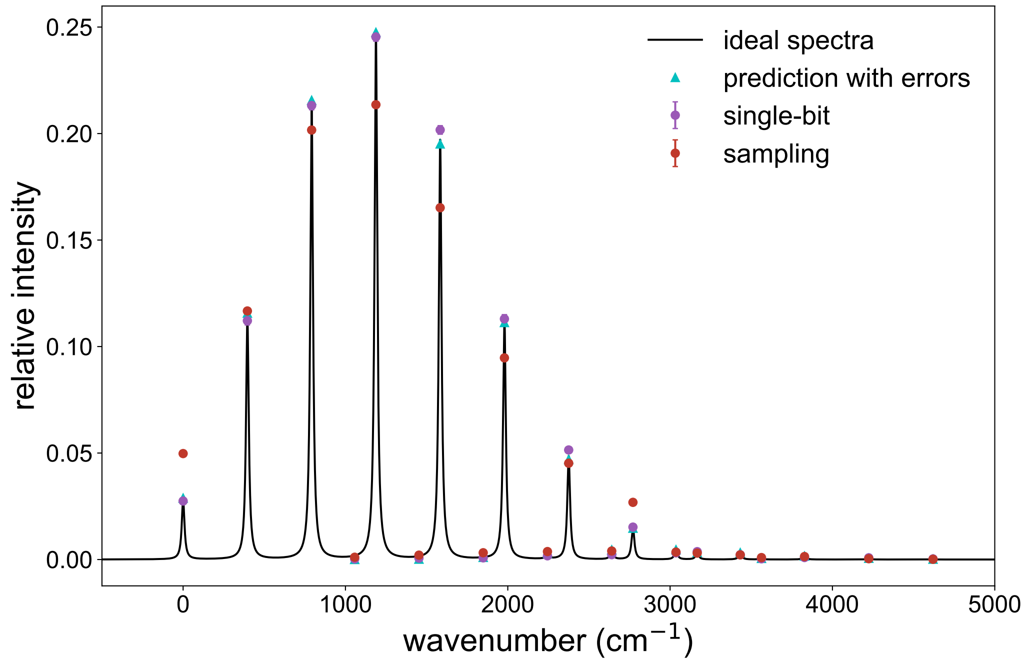

FIG. 7. Photoionization of sulfur dioxide to the cation starting in the vibrationless state $n = 0$, $m = 0$.

	$SO_2 \xrightarrow{h\nu} SO_2^+ + e^-$ starting in $(n = 0, m = 0)$			
(n', m')	Classically calculated	Master equation simulation	Single-bit extraction	Sampling
(0,0)	2.82E-02	2.88E-02	0.0275 ± 0.0009	0.0497 ± 0.0003
(0,1)	1.14E-01	1.15E-01	0.112 ± 0.002	0.1167 ± 0.0005
(0,2)	2.13E-01	2.15E-01	0.213 ± 0.002	0.2017 ± 0.0006
(0,3)	2.47E-01	2.47E-01	0.245 ± 0.002	0.2136 ± 0.0006
(0,4)	1.97E-01	1.95E-01	0.202 ± 0.002	0.1652 ± 0.0006
(0,5)	1.14E-01	1.11E-01	0.113 ± 0.002	0.0947 ± 0.0005
(0,6)	4.85E-02	4.72E-02	0.051 ± 0.001	0.0452 ± 0.0003
(0,7)	1.54E-02	1.48E-02	0.0152 ± 0.0007	0.0268 ± 0.0003
(0,8)	3.57E-03	3.38E-03	0.0037 ± 0.0004	0.00302 ± 9E-05
(0,9)	5.68E-04	5.28E-04	0.0003 ± 0.0002	0.00091 ± 5E-05
(1,0)	9.40E-06	2.89E-05	0.0003 ± 0.0001	0.00108 ± 5E-05
(1,1)	4.35E-05	1.53E-04	0.0007 ± 0.0002	0.00206 ± 7E-05
(1,2)	7.70E-04	9.82E-04	0.0008 ± 0.0002	0.00318 ± 9E-05
(1,3)	2.67E-03	2.84E-03	0.0017 ± 0.0003	0.00374 ± 0.0001
(1,4)	4.54E-03	4.53E-03	0.0023 ± 0.0003	0.004 ± 0.0001
(1,5)	4.78E-03	4.60E-03	0.0031 ± 0.0003	0.0035 ± 9E-05
(1,6)	3.44E-03	3.22E-03	0.0022 ± 0.0003	0.00219 ± 7E-05
(1,7)	1.76E-03	1.62E-03	0.0009 ± 0.0002	0.0014 ± 6E-05
(1,8)	6.53E-04	5.89E-04	0.0008 ± 0.0002	0.00038 ± 3E-05
(1,9)	1.73E-04	1.54E-04	0.0003 ± 9E-05	0.00011 ± 2E-05

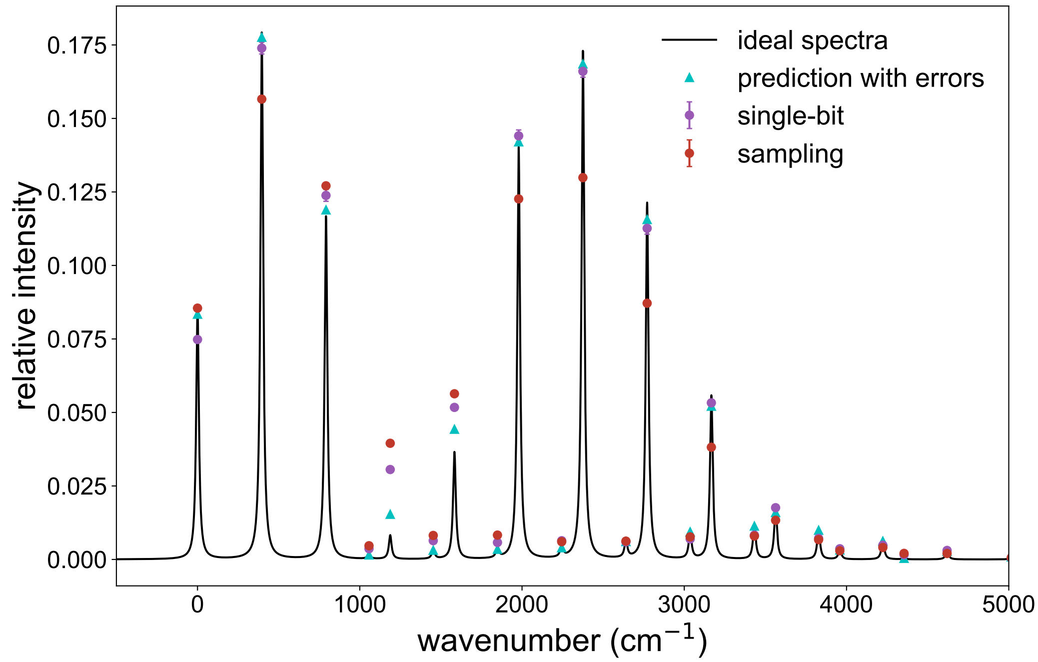

FIG. 8. Photoionization of sulfur dioxide to the cation starting with zero quanta in the symmetric-stretching mode and one quantum in the bending mode $n = 0$, $m = 1$.

	$SO_2 \xrightarrow{h\nu} SO_2^+ + e^-$ starting in $(n = 0, m = 1)$			
(n', m')	Classically calculated	Master equation simulation	Single-bit extraction	Sampling
(0,0)	8.52E-02	8.36E-02	0.075 ± 0.001	0.0855 ± 0.0005
(0,1)	1.79E-01	1.78E-01	0.174 ± 0.002	0.1566 ± 0.0006
(0,2)	1.17E-01	1.19E-01	0.124 ± 0.002	0.1271 ± 0.0006
(0,3)	8.11E-03	1.50E-02	0.0306 ± 0.0009	0.0395 ± 0.0003
(0,4)	3.64E-02	4.42E-02	0.052 ± 0.001	0.0564 ± 0.0004
(0,5)	1.40E-01	1.42E-01	0.144 ± 0.002	0.1226 ± 0.0006
(0,6)	1.73E-01	1.69E-01	0.166 ± 0.002	0.1299 ± 0.0006
(0,7)	1.21E-01	1.16E-01	0.113 ± 0.002	0.0872 ± 0.0005
(0,8)	5.56E-02	5.22E-02	0.053 ± 0.001	0.0382 ± 0.0003
(0,9)	1.74E-02	1.60E-02	0.0176 ± 0.0007	0.0133 ± 0.0002
(0,10)	3.62E-03	3.24E-03	0.0036 ± 0.0004	0.00296 ± 9E-05
(0,11)	4.51E-04	3.96E-04	0.0016 ± 0.0003	0.00206 ± 8E-05
(1,0)	1.68E-03	1.55E-03	0.0037 ± 0.0003	0.0047 ± 0.0001
(1,1)	3.27E-03	3.16E-03	0.0064 ± 0.0005	0.0082 ± 0.0002
(1,2)	3.48E-03	3.48E-03	0.0058 ± 0.0004	0.0083 ± 0.0002
(1,3)	3.89E-03	3.99E-03	0.0064 ± 0.0004	0.006 ± 0.0001
(1,4)	5.95E-03	6.09E-03	0.006 ± 0.0004	0.0062 ± 0.0001
(1,5)	9.44E-03	9.38E-03	0.007 ± 0.0005	0.0077 ± 0.0001
(1,6)	1.18E-02	1.14E-02	0.0083 ± 0.0005	0.008 ± 0.0001
(1,7)	1.07E-02	9.95E-03	0.0072 ± 0.0005	0.0067 ± 0.0001
(1,8)	6.90E-03	6.24E-03	0.0048 ± 0.0004	0.0041 ± 0.0001
(1,9)	3.18E-03	2.79E-03	0.0031 ± 0.0003	0.00203 ± 8E-05
(1,10)	1.03E-03	8.79E-04	0.0005 ± 0.0001	0.00061 ± 4E-05
(1,11)	2.26E-04	1.86E-04	4E-05 ± 6E-05	0.00035 ± 3E-05

[1] M. J. Frisch, G. W. Trucks, H. B. Schlegel, G. E. Scuseria, M. A. Robb, J. R. Cheeseman, G. Scalmani, V. Barone, G. A. Petersson, H. Nakatsuji, X. Li, M. Caricato, A. V. Marenich, J. Bloino, B. G. Janesko, R. Gomperts, B. Mennucci, H. P. Hratchian, J. V. Ortiz, A. F. Izmaylov, J. L. Sonnenberg, D. Williams-Young, F. Ding, F. Lipparini, F. Egidi, J. Goings, B. Peng, A. Petrone, T. Henderson, D. Ranasinghe, V. G. Zakrzewski, J. Gao, N. Rega, G. Zheng, W. Liang, M. Hada, M. Ehara, K. Toyota, R. Fukuda, J. Hasegawa, M. Ishida, T. Nakajima, Y. Honda, O. Kitao, H. Nakai, T. Vreven, K. Throssell, J. A. Montgomery, Jr., J. E. Peralta, F. Ogliaro, M. J. Bearpark, J. J. Heyd, E. N. Brothers, K. N. Kudin, V. N. Staroverov, T. A. Keith, R. Kobayashi, J. Normand, K. Raghavachari, A. P. Rendell, J. C. Burant, S. S. Iyengar, J. Tomasi, M. Cossi, J. M. Millam, M. Klene, C. Adamo, R. Cammi, J. W. Ochterski, R. L. Martin, K. Morokuma, O. Farkas, J. B. Foresman, and D. J. Fox, Gaussian 16, Revision A.03, Gaussian, Inc., Wallingford, CT, 2016.

[2] V. A. Mozhayskiy and A. I. Krylov, ezSpectrum (ver. 3.0), downloaded January 2019 from http://iopenshell.usc.edu/downloads, 2014.

[3] T. H. Dunning, Jr., Gaussian Basis Sets for Use in Correlated Molecular Calculations. I. The Atoms Boron Through Neon and Hydrogen. *J. Chem. Phys.* 90, 1007-1023 (1989).

[4] R. A. Kendall, T. H. Dunning, Jr., R. J. Harrison, Electron Affinities of the First-Row Atoms Revisited. Systematic Basis Sets and Wave Functions. *J. Chem. Phys.* 96, 6796-6806 (1992).

[5] D. E. Woon, T. H. Dunning, Jr., Gaussian Basis Sets for Use in Correlated Molecular Calculations. III. The Atoms Aluminum through Argon. *J. Chem. Phys.* 98, 1358-1371 (1993).

[6] M. Reck, A. Zeilinger, H. J. Bernstein, P. Bertani. Experimental realization of any discrete unitary operator. *Phys. Rev. Lett.* 73, 58-61 (1994).

[7] George Cybenko. Reducing Quantum Computations to Elementary Unitary Operations, *Computing in Science* & *Engineering* 3, 27 (2001).

[8] J. Huh, G. G. Guerreschi, B. Peropadre, J. R. McClean, A. Aspuru-Guzik. Boson sampling for molecular vibronic spectra. *Nature Photonics.* 9, 615–620 (2015).

[9] Y. Shen, Y. Lu, K. Zhang, J. Zhang, S. Zhang, J. Huh, K. Kim. Quantum optical emulation of molecular vibronic spectroscopy using a trapped-ion device. *Chem. Sci.* 9, 836–840 (2018).

[10] Y. Y. Gao, B. J. Lester, Y. Zhang, C. Wang, S. Rosenblum, L. Frunzio, L. Jiang, S. M. Girvin, R. J. Schoelkopf. Programmable Interference between Two Microwave Quantum Memories. *Phys. Rev. X.* 8, 021073 (2018).

[11] Y. Zhang, B. J. Lester, Y. Y. Gao, L. Jiang, R. J. Schoelkopf, S. M. Girvin. Engineering bilinear mode coupling in circuit QED: Theory and experiment. *Phys. Rev. A.* 99, 012314 (2019).

[12] J. Koch, T. M. Yu, J. Gambetta, A. A. Houck, D. I. Schuster, J. Majer, A. Blais, M. H. Devoret, S. M. Girvin, R. J. Schoelkopf. Charge-insensitive qubit design derived from the Cooper pair box. *Phys. Rev. A.* 76, 042319 (2007).

[13] K. S. Chou, "Teleported operations between logical qubits in circuit quantum electrodynamics", thesis, Yale University (2018).

[14] S. S. Elder, C. S. Wang, P. Reinhold, C. T. Hann, K. S. Chou, B. J. Lester, S. Rosenblum, L. Frunzio, L. Jiang, R. J. Schoelkopf. High-fidelity measurement of qubits encoded in multilevel superconducting circuits. *Phys. Rev. X* (Accepted) (2019).